

Stress and fabric for polydisperse, frictionless, dense 2D granular media

M. Madadi*, S. M. Peyghoon

Department of Physics, Faculty of Basic Sciences, University of Mazandaran, Babolsar, Iran

S. Luding*

Particle Technology, DelftChemTech, TU Delft, Julianalaan 136, 2628 BL Delft, The Netherlands

* Part of the work was performed at: *ICP, Pfaffenwaldring 27, 70569 Stuttgart, Germany*

ABSTRACT For fabric and stress tensor, correlations of microscopic quantities are studied and the influence of the particle size probability distribution function is isolated from that of other quantities. Based on the observations that the covered surface area and the average force per contact are (almost) size-independent, we show that fabric and stress can be factorized into products of some averaged quantities (like coordination number, particle radius, or contact force), and dimensionless correction factors, which depend *only* on moments of the particle size distribution function. Numerical simulations are in proper agreement with the theoretical predictions for moderately wide size distributions.

1 INTRODUCTION

On the microscopic level, a granular assembly of frictionless, spherical (disk) particles consists of a contact network, with the so-called branch vectors connecting the centers of two particles in contact, and the corresponding forces acting parallel to the branch vector. Theoretical predictions are possible for this (simple) special case of the more realistic assembly of frictional, non-spherical granular particles.

The fabric tensor of polydisperse granular 2D spheres (disks) has been studied, see (Madadi et al. 2004) and references therein. The trace of the fabric tensor factorizes into three contributions: (i) the volume fraction, (ii) the mean coordination number, and (iii) a dimensionless correction factor g_2 , which only depends on the particle size distribution function. These results are based on the basic assumption that for all particles, the fraction of surface shielded by other particles is independent of their radius. As long as the size distribution function is not too wide, the theory is in very good agreement with simulations, and the first three moments of the distribution function are sufficient to determine g_2 .

The main goal of this study is to calculate, in the same spirit, the analytical expression for the trace of the stress, i.e. for the isotropic pressure, for polydisperse particle packings in two dimensions (2D). First, it is assumed that the trace of the macroscopic stress tensor is – in average – independent of the particle size. This is consistent with the constant stress con-

dition (the divergence of the stress should vanish) for static equilibrium. Second, the stress is factorized, involving the assumption of a size independent, scaled contact force. Both fabric and stress tensor are introduced in section 2, the results are discussed in section 3, before conclusions are presented in section 4.

2 FABRIC AND STRESS TENSORS

Besides the structure of a static packing of powders and grains, one of the most important quantities of interest is the stress tensor. The fabric tensor describes the direction dependent probability to find contacts, while the stress tensor gives the same probability but weighted by the particle size and the force acting at such contacts.

2.1 Single particle definitions

The expressions for the components of the fabric tensor are for a single particle $F_{\alpha\beta}^p = \frac{1}{a_p^2} \sum_{c=1}^{C^p} l_{\alpha}^{pc} l_{\beta}^{pc}$, with l_{α}^{pc} , the components of the branch-vector from the center of particle p to contact c , and a_p , the particle radius. The single-particle fabric is normalized such that its trace is the coordination number, i.e., the number of contacts, C^p , of particle p .

The stress tensor for a single particle in a granular assembly is $\sigma_{\alpha\beta}^p = \frac{1}{V_p} \sum_{c=1}^{C^p} l_{\alpha}^{pc} F_{\beta}^{pc}$, with F_{β}^{pc} , the components of the force acting at contact c on particle p , with volume $V_p = \pi h a_p^2$, and disk-height h . In 2D, the pressure is the isotropic stress: $p = \sigma_{\alpha\alpha}/2$.

Using the average force $\overline{F}(a) = \int_0^\infty F p_a(F) dF$, with the probability $p_a(F) dF$ to find a force (for particles of radius a) in the range between F and $F + dF$, the trace of the stress reduces to $\sigma_{\alpha\alpha}^p = a_p \overline{F}(a_p) C^p / V_p$. Note that not only $p_a(F)$ is a distribution with exponential tail and peculiar system- and configuration dependent properties for short range forces (Radjai & Wolf 1998; Snoeijer et al. 2003), but also the averaged particle stresses occur with rather wide distribution. However, this point will not be discussed further in this paper.

2.2 Many particle definitions

In the many particle case, the trace of the averaged fabric tensor is $\langle F_{\alpha\alpha} \rangle_V = \frac{1}{V} \sum_{p \in V} V_p C^p$, and the trace of the averaged stress tensor is

$$\langle \sigma_{\alpha\alpha} \rangle_V = \frac{1}{V} \sum_{p \in V} \sum_{c=1}^{C^p} I_{\alpha}^{pc} F_{\beta}^{pc} = \frac{1}{V} \sum_{p \in V} V_p \sigma_{\alpha\alpha}^p, \quad (1)$$

see (Lätzel et al. 2000; Madadi et al. 2004) and references therein.

Assume a polydisperse distribution of particle radii with probability $f(a) da$ to find particles with radius between a and $a + da$, and with normalization condition $\int_0^\infty da f(a) = 1$, and the moments $\overline{a^k} = \int_0^\infty da a^k f(a)$. Therefore, considering the continuous limit of the fabric sum and the stress sum, Eq. (1), for a large number N of particles within volume V , one has the integrals:

$$\langle F_{\alpha\alpha} \rangle_V = \frac{N}{V} \int_0^\infty da \pi h a^2 C(a) f(a), \quad (2)$$

and

$$\langle \sigma_{\alpha\alpha} \rangle_V = \frac{N}{V} \int_0^\infty da \pi h a^2 \sigma_{\alpha\alpha}^p(a) f(a), \quad (3)$$

with the average coordination number $C(a)$, and the stress $\sigma_{\alpha\alpha}^p(a)$ of particles with radius a . In Eq. (3), a certain stress was assumed for particles of size a , however, particles with different sizes can have different stresses.

2.3 Fabric and polydispersity

When trying to simplify Eq. (2), one can distinguish three different cases: (i) constant coordination number for all particles, (ii) the monodisperse case with constant a , and (iii) the general situation of arbitrary coordination number and polydisperse particles. In a polydisperse assembly, in general, one can neither assume (i) or (ii), such that Eq. (2) typically does not just factorize to $(N/V) \pi h \overline{a^2} \overline{C}$. The problem is thus to determine the integral in Eq. (2) as a function of the size distribution function.

The trace of the fabric can be evaluated using an approach similar to the one proposed by (Ouchiyama & Tanaka 1981), and used by (Madadi et al. 2004):

Assume that a reference particle with radius a is surrounded by identical particles of mean radius \bar{a} . First, we are interested in that part of the reference particle's surface that is covered or shielded by contact partners, as sketched in Fig. 1.

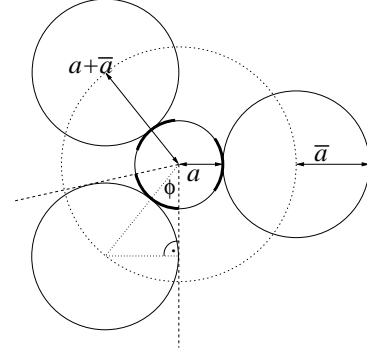


Figure 1. Schematic graph of a central particle with radius a (small solid circle), surrounded by identical particles with radius equal to the mean radius \bar{a} (large solid circles). The 2D surface area of the center particle, shielded by the lower sphere, is indicated as an angle plotted with a thick solid lines.

The angle covered by a particle with radius \bar{a} on a particle of radius a is

$$\phi(a) = \arcsin\left(\frac{\bar{a}}{a + \bar{a}}\right) = \arcsin\left(\frac{1}{\epsilon + 2}\right), \quad (4)$$

where $\epsilon = a/\bar{a} - 1$ is a small quantity for narrow size distributions and thus quantifies the deviation from the monodisperse situation. Using the shielded angle from Eq. (4), the linear compacity $c_s = 2\phi(a)C(a)/2\pi$, of the reference particle defines the total fraction of its surface, which is shielded by other particles. The basic assumption for the following analysis is that c_s is independent of a . Thus, using $C(a) = \pi c_s / \phi(a)$, the expected mean coordination number becomes $\overline{C} = \int_0^\infty da C(a) f(a) = \pi c_s q_0$, with $q_0 = \int_0^\infty da f(a) / \phi(a)$, the zero-th moment of the modified distribution function $f(a) / \phi(a)$.

The trace of the fabric tensor is thus $\langle F_{\alpha\alpha} \rangle_V = \overline{C} \nu g_2$, with the volume fraction $\nu = N \pi h \overline{a^2} / V$, and $g_2 = \langle a^2 \rangle_g / \overline{a^2}$, with the (normalized) second moment of the modified size distribution $f(a) / \phi(a)$, abbreviated as $\langle a^2 \rangle_g = (1/q_0) \int_0^\infty da a^2 f(a) / \phi(a)$; see (Madadi et al. 2004) for details.

2.4 Stress and polydispersity

For the stress tensor, we observe from simulations with moderately wide size distributions, that the average particle stress is independent of the particle size, $\overline{\sigma_{\alpha\alpha}^p} = \sigma_{\alpha\alpha}^p(a)$. Eq. (3) then simplifies to

$$\langle \sigma_{\alpha\alpha} \rangle_V = (N/V) \pi h \overline{a^2} \overline{\sigma_{\alpha\alpha}^p} = \nu \overline{\sigma_{\alpha\alpha}^p}. \quad (5)$$

Extracting (the constant) c_s from the stress integral yields $\langle \sigma_{\alpha\alpha} \rangle_V = (N/V) \overline{C} \langle a \overline{F}(a) \rangle_g$, with $\langle a \overline{F}(a) \rangle_g = (1/q_0) \int_0^\infty da a \overline{F}(a) f(a) / \phi(a)$, the product of a and $\overline{F}(a)$ averaged over the normalized, modified size distribution $f(a) / \phi(a)$. This maybe not appropriate

for a factorization in terms of all averaged micro-quantities, but it allows to express the stress in the same way as the fabric: $\langle \sigma_{\alpha\alpha} \rangle_V = \overline{C} \nu g_{1F} / (\pi h) = (N/V) \overline{C} \overline{a^2} g_{1F}$, with $g_{1F} = \langle a \overline{F}(a) \rangle_g / \overline{a^2}$. This is especially important in a situation, where the forces are measured experimentally as a function of the particle radii and can be used for this averaging.

2.5 Stress as function of the average normal force

From our simulations, see below, we observe that $\overline{F}(a)/C(a) \propto \overline{F}(a)\phi(a) \approx \overline{F}\phi(\overline{a}) = \overline{F}\pi/6$, such that

$$\langle \sigma_{\alpha\alpha} \rangle_V = \frac{\nu \overline{C} \overline{F} \overline{a} a_1}{6 h \overline{a^2}} = \frac{N}{V} \overline{C} \overline{F} \overline{a} a_1, \quad (6)$$

with

$$a_1 = \frac{\pi}{6 q_0 \overline{a}} \int_0^\infty da a f(a) / \phi^2(a), \quad (7)$$

the normalized first moment of the modified distribution $f(a)/\phi^2(a)$, which cannot be related to the previous correction factors.

2.6 Narrow size distributions

In the limit of a narrow size distribution, by Taylor expansion to first order in ϵ (corresponding to a Taylor expansion around $a = \overline{a}$), one obtains:

$$\frac{1}{\phi(a)} \approx \frac{6}{\pi} \left(1 - \frac{\sqrt{3}}{\pi} + \frac{\sqrt{3}}{\pi} \frac{a}{\overline{a}} \right), \quad (8)$$

and

$$\frac{1}{\phi^2(a)} \approx \left(\frac{6}{\pi} \right)^2 \left(1 - \frac{2\sqrt{3}}{\pi} + \frac{2\sqrt{3}}{\pi} \frac{a}{\overline{a}} \right). \quad (9)$$

The inverse of Eq. (4) and its Taylor expansion in Eq. (8) have less than one per-cent error in the range $-0.5 < \epsilon < 1.5$ (or $0.5 < a/\overline{a} < 2.5$) (Madadi et al. 2004), even though the agreement for Eq. (9) is not as good. With $q_0 \approx 6/\pi$, one obtains

$$g_2 \approx 1 + \frac{\sqrt{3}}{\pi} \left(\frac{\overline{a^3}}{\overline{a} \overline{a^2}} - 1 \right), \quad (10)$$

see (Madadi et al. 2004), and

$$a_1 \approx 1 + \frac{2\sqrt{3}}{\pi} \left(\frac{\overline{a^2}}{\overline{a}^2} - 1 \right), \quad (11)$$

where only the first two moments of the size distribution are involved. Note the coincidence, $\nu_{\max} = \pi/(2\sqrt{3})$, the close-packing density for a regular triangular lattice in 2D (Luding 2002).

3 RESULTS

In this section, we contrast our theory to numerical data for a few special cases with rather small averaging volumes with about 100-400 particles and two size distributions, a narrow and a rather wide one. In the following subsection, the size distribution and its consequences for the correction factor a_1 are discussed, before the simulation results are presented in the following.

3.1 Uniform polydisperse size distribution

In a uniform polydisperse system, a special case of polydisperse systems, the radius of the particles is distributed uniformly between $(1 - w_0)\overline{a}$ and $(1 + w_0)\overline{a}$, where $2w_0\overline{a}$ is the width of size-distribution function $f(a)$ (Madadi et al. 2004). It is straightforward to compute the contributions to the correction factor, like $\overline{a^2} = \overline{a^2}(1 + w_0^2/3)$, and

$$a_1 = \frac{\pi}{6} \frac{\int_{1-w_0}^{1+w_0} \arcsin^{-2}\left(\frac{1}{1+x}\right) x dx}{\int_{1-w_0}^{1+w_0} \arcsin^{-1}\left(\frac{1}{1+x}\right) dx}. \quad (12)$$

The polydispersity correction, Eq. (12), for $w_0 = 1/2$, leads to $a_1 = 1.116$, while from the approximation, Eq. (11), one gets $a_1 \approx 1.092$, in good agreement. For much wider size distributions, for example $w_0 = 0.9$, one obtains $a_1 = 1.38$, and from the approximation $a_1 \approx 1.30$, still less than ten per-cent deviation.

3.2 Numerical Results

To test the theory from the previous section, all necessary quantities are computed in average over parts of the simulation volume. For the simulations, a soft-sphere molecular dynamics with linear visco-elastic normal contact forces (with stiffness k_n) is used (Lätzel et al. 2000; Madadi et al. 2004; Luding 2004). First, about 600 particles with radii drawn from a uniform polydisperse distribution, are put in a bi-axial box, which is compressed until a desired volume fraction is reached. In the case of the narrow ($w_0 = 0.5$) and wide ($w_0 = 0.9$) size distributions, the target volume fractions are $\nu = 0.93$ and $\nu = 0.86$, respectively. The density for the narrow size distribution is rather large complementing our previous results (Madadi et al. 2004). After the system is relaxed to a state where the kinetic energy is much smaller than the potential energy, the averages are taken.

For averaging, the system is divided into subsystems distant from the walls. More specific, we perform one average where only the center volume with side-length 0.8 and thus area 0.64 of the total volume is used for the average. In a second series of averages, several (overlapping) averaging volumes with side-length 0.4 and thus area 0.16 of the total are used. These two situations will be referred to as large and small averaging volume, respectively. In each subsystem, we calculate the average of the averaged trace of the fabric and stress tensors, the averaged force, \overline{F} , the average of the contact number, \overline{C} , the averages of the moments, $\overline{a^k}$, as well as the density, N/V , and the volume fraction.

To check whether the combination $\overline{F}(a)\phi(a)$, which corresponds also to the averaged force per contact, $\overline{F}(a)/C(a)$, is in fact constant as assumed, this scaled force is plotted in Fig. 2, for size distributions with $w_0 = 0.5$ and $w_0 = 0.9$ (four different realizations each – obtained from different initial conditions).

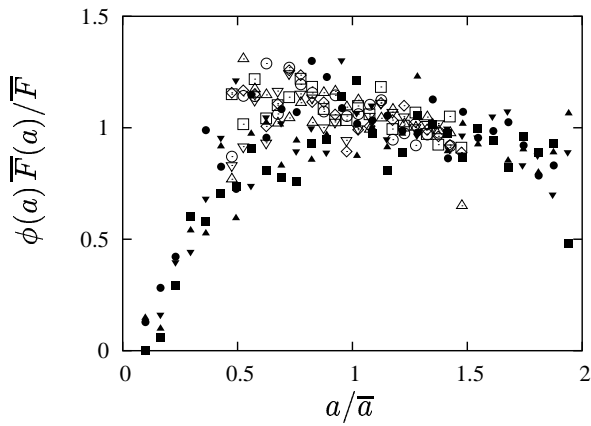


Figure 2. Scaled force for different simulations with narrow (open symbols) and wide (solid symbols) size distributions.

The term $\overline{F}(a)\phi(a)$ is almost constant for the narrow size distribution; for the wider size distribution, an overproportional large number of very small particles is obtained which behave as so-called “rattlers”, sitting in pores between other particles and not contributing with forces to the structure. Finally, a slow decrease of $\overline{F}(a)\phi(a)$ with the particle size is noted.

Fig. 3 shows the predicted, factorized stress from Eq. (6) plotted against the trace of the stress tensor from direct averaging. The data are close to the solid (identity) line as expected from theory – for the narrow and also for the wide size distribution – with correction factors $a_1 = 1.09$ and $a_1 = 1.30$, respectively. Note that we used the approximated correction factor a_1 from Eq. (11) here, since the exact expression shows, interestingly, somewhat less good agreement.

4 CONCLUSION

In conclusion, the isotropic fabric factorizes into volume fraction coordination number and a correction factor, while the isotropic stress factorizes into products of the density, particle size, coordination number, mean force and correction factor. The polydispersity of the size distribution is taken into account via these (non-dimensional) correction factors, which only depend on moments of the size distribution – in first order approximation. For both fabric and strain reasonable agreement between theory and numerical simulations was observed.

Our correction factors rely on a series of assumptions and are therefore not perfect. For both stress and fabric corrections in the range of 5-30 per-cent are predicted and the agreement between theory and simulations is typically much better than 1-4 per-cent, respectively. Thus, improving the quality of the assumptions made (the assumptions on constant covered area fraction or force per contact of the center particle surrounded only by representative mean-sized particles) is one goal for future research. However, also the question about the usefulness of the present theory for anisotropic and frictional systems is of interest. Similar studies are in progress in three-dimensional sys-

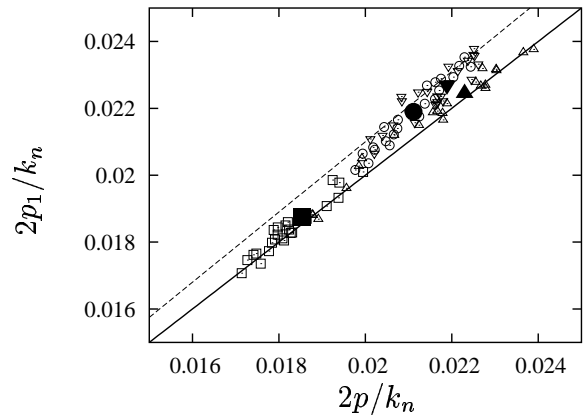
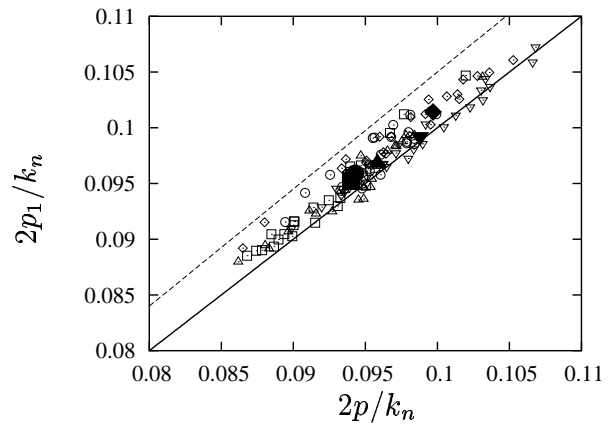


Figure 3. Predicted trace of stress, $2p := (N/V)\overline{C}\overline{F}\overline{a}a_1$, plotted against the averaged trace of the stress tensor, $2p := \langle \sigma_{\alpha\alpha} \rangle_V$, both plotted in units of the contact spring-stiffness k_n . The solid line gives the theoretical prediction while the dashed line indicates a five per-cent error margin. Solid and open symbols correspond to the large and small averaging volumes, respectively.

tems, however, an experimental check of our predictions is still missing in 2D and 3D as well.

ACKNOWLEDGEMENTS

The financial support of the Deutsche Forschungsgemeinschaft (DFG) is acknowledged. M. M. would like to acknowledge UMZ for support of the research.

REFERENCES

- Lätzel, M., Luding, S., & Herrmann, H. J. 2000. Macroscopic material properties from quasi-static, microscopic simulations of a two-dimensional shear-cell. *Granular Matter* 2(3): 123–135. cond-mat/0003180.
- Luding, S. 2002. Liquid-solid transition in bi-disperse granulates. *Advances in Complex Systems* 4(4): 379–388.
- Luding, S. 2004. Micro-macro transition for anisotropic, frictional granular packings. *Int. J. Sol. Struct.* 41: 5821–5836.
- Madadi, M., Tsoungui, O., Lätzel, M., & Luding, S. 2004. On the fabric tensor of polydisperse granular media in 2d. *Int. J. Sol. Struct.* 41(9-10): 2563–2580.
- Ouchiyama, N. & Tanaka, T. 1981. Porosity of a mass of solid particles having a range of sizes. *Ind. Eng. Chem. Fund.* 20(1): 66–71.
- Radjai, F. & Wolf, D. E. 1998. The origin of static pressure in dense granular media. *Granular Matter* 1: 3–8.
- Snoeijer, J. H., van Hecke, M., Somfai, E., & van Saarloos, W. 2003. Force and weight distributions in granular media: Effects of contact geometry. *Phys. Rev. E* 67: 030302(R). cond-mat/0204277.